

GIANT METREWAVE RADIO TELESCOPE DETECTION OF TWO NEW HI 21CM ABSORBERS AT $Z \approx 2$

N. KANEKAR¹,

Draft version January 23, 2020

ABSTRACT

I report the detection of HI 21cm absorption in two high column density damped Lyman- α absorbers (DLAs) at $z \approx 2$ using new wide-band 250 – 500 MHz receivers onboard the Giant Metrewave Radio Telescope. The integrated HI 21cm optical depths are $0.85 \pm 0.16 \text{ km s}^{-1}$ (TXS1755+578) and $2.95 \pm 0.15 \text{ km s}^{-1}$ (TXS1850+402). For the $z = 1.9698$ DLA towards TXS1755+578, the difference in HI 21cm and C I profiles and the weakness of the radio core suggest that the HI 21cm absorption arises towards radio components in the jet, and that the optical and radio sightlines are not the same. This precludes an estimate of the DLA spin temperature. For the $z = 1.9888$ DLA towards TXS1850+402, the absorber covering factor is likely to be close to unity, as the background source is extremely compact, with all the 5 GHz emission arising from a region of size $\leq 1.4 \text{ mas}$. This yields a DLA spin temperature of $T_s = (372 \pm 18) \times (f/1.0) \text{ K}$, lower than typical T_s values in high- z DLAs. This low spin temperature and the relatively high metallicity of the $z = 1.9888$ DLA ($[\text{Zn}/\text{H}] = (-0.68 \pm 0.04)$) are consistent with the anti-correlation between metallicity and spin temperature that has been earlier found in damped Lyman- α systems.

Subject headings: atomic processes — galaxies: high-redshift — quasars: absorption lines

1. INTRODUCTION

HI 21cm absorption studies have long been used to study neutral hydrogen (HI) in both galaxies fortuitously located along the line of sight to background radio-loud quasars and gas associated with active galactic nuclei. In the case of absorption-selected galaxies at high redshifts, the damped Lyman- α absorbers (DLAs; Wolfe et al. 2005), the HI 21cm optical depth can be combined with the HI column density (inferred from the Lyman- α absorption profile) to yield the spin temperature of the neutral gas along the sightline (e.g. Kanekar & Briggs 2004). HI 21cm absorption studies thus provide one of the few direct probes of physical conditions in the neutral gas in high-redshift DLAs (e.g. Carilli et al. 1996; Chengalur & Kanekar 2000; Kanekar & Chengalur 2003), complementing optical and ultraviolet estimates of elemental abundances, molecular fractions, dust depletions, kinematic widths, etc, from observations of low-ionization metal and molecular hydrogen lines (e.g. Pettini et al. 1994; Prochaska et al. 2003; Noterdaeme et al. 2008; Rafelski et al. 2012).

Early HI 21cm absorption studies of high-redshift DLAs suggested that conditions in the neutral interstellar medium in these galaxies were different from those in the Milky Way. The few high- z DLAs with HI 21cm absorption studies were found to have relatively high spin temperatures ($T_s \gtrsim 1000 \text{ K}$), nearly five times higher than typical values in the Milky Way (e.g. Dickey et al. 1978; Wolfe & Davis 1979; Wolfe et al. 1982, 1985; Braun & Walterbos 1992; Carilli et al. 1996; de Bruyn et al. 1996; Briggs et al. 1997; Kanekar & Chengalur 1997). Unfortunately, the poor low-frequency coverage of radio telescopes meant that such studies were only possible in a handful of DLAs at $z \gtrsim 2$. To make matters worse, few DLAs were known at low redshifts, due to which there were also hardly any T_s measurements in DLAs at $z < 1$.

The situation has changed significantly over the last decade,

with the advent of the Green Bank Telescope (GBT) and the Giant Metrewave Radio Telescope (GMRT) which combine high sensitivity with excellent low-frequency radio coverage. There are now more than 50 DLAs at all redshifts with HI 21cm absorption studies, nearly 40 of which have estimates of the spin temperature after correcting for the absorber covering factor (see Kanekar et al. 2014, and references therein). Targeted Lyman- α spectroscopy of strong MgII $\lambda 2796$ absorbers (Rao & Turnshek 2000; Rao et al. 2006) and radio-loud quasars (Ellison et al. 2001, 2008; Jorgenson et al. 2006) have yielded new samples of DLAs at all redshifts for follow-up HI 21cm absorption studies. Conversely, more than twenty-five redshifted HI 21cm absorbers at $z < 1.7$ have been identified from direct spectroscopy of strong MgII $\lambda 2796$ absorbers (e.g. Lane et al. 1998; Lane & Briggs 2002; Kanekar et al. 2009b; Gupta et al. 2007, 2009, 2012). Follow-up Lyman- α spectroscopy of some of these systems has provided estimates of the HI column density, and hence, of the absorber spin temperature (Ellison et al. 2012). Finally, high-resolution optical spectroscopy of systems with HI 21cm absorption studies have been used to infer their gas-phase metallicities, dust depletions, etc, for comparison with the measured spin temperatures (e.g. Kanekar et al. 2009c, 2014; Srianand et al. 2012; Ellison et al. 2012).

Based on the above studies, it is now apparent that the spin temperature distribution in DLAs is significantly different from that in the Milky Way, with DLAs having typically higher spin temperatures (Kanekar & Chengalur 2003; Kanekar et al. 2014). The anti-correlation detected between spin temperatures and metallicities in DLAs indicates that their high T_s values arise due to larger fractions of the warm phase of neutral hydrogen in the absorbers, probably due to fewer radiative cooling routes at their typically-low metallicities (Kanekar & Chengalur 2001; Kanekar et al. 2009c, 2014). DLA spin temperatures also show redshift evolution: absorbers at $z \gtrsim 2.4$ have both fewer detections of HI 21cm absorption and higher spin temperatures than systems at $z \lesssim 2.4$, again due to their smaller cold gas fractions (Carilli et al. 1996; Chengalur & Kanekar 2000;

¹ Ramanujan Fellow, National Centre for Radio Astrophysics, TIFR, Ganeshkhind, Pune - 411007, India; nkanekar@ncra.tifr.res.in

Kanekar & Chengalur 2003; Kanekar et al. 2014).

Despite the recent progress in the field, an important lacuna remains the paucity of *detections* of HI 21cm absorption at high redshifts, $z \gtrsim 2$. There are, at present, only seven detections of HI 21cm absorption in DLAs at $z \gtrsim 2$ (Wolfe et al. 1982, 1985; Kanekar et al. 2006, 2007, 2013; York et al. 2007; Srianand et al. 2012). While HI 21cm non-detections provide lower limits to T_s , which are useful in testing its redshift evolution, a detailed understanding of the evolution of the spin temperature and its relation with quantities like metallicity, dust depletion and star formation rate, as well as modeling of local physical conditions in the gas, critically require detections of HI 21cm absorption. HI 21cm line detections at high redshifts are also needed to use the lines in conjunction with ultraviolet resonance lines to probe the possibility of fundamental constant evolution (Wolfe et al. 1976; Kanekar et al. 2010; Rahmani et al. 2012). Until now, the GBT has been the only telescope providing wide frequency coverage below 1 GHz; unfortunately, the GBT is a single dish and hence more susceptible to the terrestrial interference that is common at these low radio frequencies. I report here two new detections of redshifted HI 21cm absorption at $z \approx 2$, first results from new wide-band 250–500 MHz receivers that are currently being installed on the GMRT.

2. OBSERVATIONS, DATA ANALYSIS AND SPECTRA

The GMRT is presently being upgraded with a new suite of receivers that will give the telescope near-seamless coverage between 120 MHz and 1437 MHz. As part of this upgrade, the present 327 MHz receivers (which covers $\approx 295 - 365$ MHz) are being replaced by wide-band cone-dipole receivers covering $\approx 250 - 500$ MHz, and with higher sensitivity than that of the earlier P-band system (Bandari et al. 2013). The initial commissioning tests of the new receivers yielded tentative detections of redshifted HI 21cm absorption in two DLAs at $z = 1.9698$ towards TXS1755+578 and $z = 1.9888$ towards TXS1850+402 (Jorgenson et al. 2006). These two DLAs were hence re-observed in July 2013 to confirm the detections of HI 21cm absorption.

The GMRT observations of the two $z \approx 2$ DLAs were carried out on 2013, July 31, using the eleven antennas equipped with the new cone-dipole receivers, and the GMRT Software Backend. Bandwidths of 1.04 MHz (TXS1850+402) and 4.17 MHz (TXS1755+578) were used for the observations, sub-divided into 512 channels, and centred at the redshifted HI 21cm line frequency (478.28 MHz for TXS1755+578 and 475.24 MHz for TXS1850+402). Observations of 3C286 and 3C48 were used to calibrate the flux density scale, and of 3C380 to calibrate the antenna bandpasses and initial antenna gains. The total on-source time was 3.5 hours for each source.

The GMRT data were analysed in “classic” AIPS, using standard procedures. After initial data editing and calibration of the antenna gains and bandpasses, about 50 channels on each target source were averaged into a “channel-0” dataset. A standard self-calibration procedure was then used to obtain the antenna gains, with a few rounds of phase-only self-calibration and 3-D imaging, followed by amplitude-and-phase self-calibration, 3-D imaging and data editing. This procedure was continued until the image did not improve on further self-calibration, and no evidence was found for bad data. In both cases, the target source was the strongest source in the field, with flux densities (measured using JMFIT) of 377.4 ± 1.3 mJy (TXS1755+578) and 650.3 ± 3.2 mJy (TXS1850+402). Neither source showed evidence of ex-

tended emission in the GMRT images. The final image was then subtracted from the calibrated spectral-line visibilities using the task UVSUB, and UVLIN then used to subtract any residual emission via a linear fit to each visibility spectrum. Finally, CVEL was used to shift the residual visibilities to the heliocentric frame. The data were then imaged and a spectrum obtained by taking a cut through the spectral cube at the location of the target sources.

The final GMRT spectra towards TXS1755+578 and TXS1850+402 are shown in the two panels of Fig. 1, with optical depth plotted versus heliocentric frequency. The spectrum towards TXS1850+402 has been Hanning-smoothed and re-sampled, and has a velocity resolution of ≈ 2.5 km s $^{-1}$, while that towards TXS1755+578 has been further boxcar-smoothed by 3 channels and re-sampled, and has a velocity resolution of ≈ 31 km s $^{-1}$. The root-mean-square (RMS) optical depth noise values on the original Hanning-smoothed and re-sampled spectra are 0.011 per 4.1 kHz channel (TXS1850+402) and 0.0092 per 16.3 kHz channel (TXS1755+578); note that significantly more data were edited out for the latter source, due to intermittent radio frequency interference. Both spectra show evidence of HI 21cm absorption, with integrated HI 21cm optical depths of 2.95 ± 0.14 km s $^{-1}$ (TXS1850+402) and 0.85 ± 0.16 km s $^{-1}$ (TXS1755+578). Note that the HI 21cm absorption towards TXS1755+578 is relatively weak, and extends across only two independent 31 km s $^{-1}$ channels. However, the feature has $> 5\sigma$ significance and was detected in both observing runs, separated by many months. It is hence likely to be real.

3. RESULTS AND DISCUSSION

For HI 21cm absorption against a compact radio source, the HI column density (N_{HI}), the HI 21cm optical depth ($\tau_{21\text{cm}}$) and the spin temperature (T_s) are related by the equation (e.g. Rohlfs & Wilson 2006)

$$N_{\text{HI}} = 1.823 \times 10^{18} (T_s/f) \int \tau_{21\text{cm}} dV, \quad (1)$$

where f is the absorber covering factor, giving the fraction of the background radio emission that is occulted by the foreground DLA. The covering factor can be estimated from very long baseline interferometry (VLBI) observations at or near the redshifted HI 21cm line frequency to determine the fraction of flux density in the compact radio core (e.g. Briggs & Wolfe 1983; Kanekar et al. 2009a, 2014). Note that a critical assumption in the above equation is that the HI column density measured along the optical sightline is the same as that along the radio sightline. The HI column densities of the DLAs towards TXS1755+578 and TXS1850+402 are $(2.51 \pm 0.15) \times 10^{21}$ and $(2.00 \pm 0.25) \times 10^{21}$, respectively. Equation 1 then yields $T_s = (1612 \pm 305) \times f$ (TXS1755+578) and $T_s = (372 \pm 18) \times f$ K (TXS1850+402). The above results are summarized in Table 1.

Unfortunately, there are at present, no low-frequency VLBI observations of TXS1755+578 and TXS1850+402 from which one might directly measure the fraction of flux density in the radio core. However, the two sources have either inverted (TXS1755+578) or flat (TXS1850+402) spectra at low frequencies; such spectra typically arise due to synchrotron self-absorption, indicating that the radio emission is very compact. One hence would expect a relatively high core fraction in both sources. In the case of TXS1850+402, VLBI observations have found all the 5 GHz emission to arise from two components both lying in a region smaller than ≈ 1.4 mas

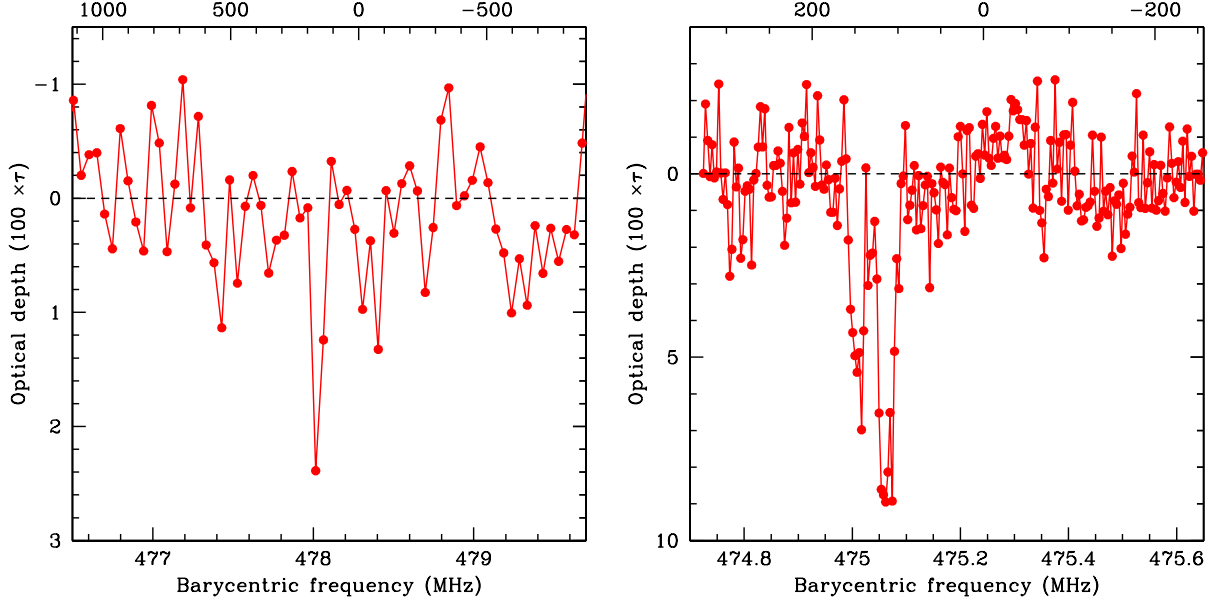


FIG. 1.— GMRT H I absorption spectra from [A] the $z = 1.9698$ DLA towards TXS1755+578 (left panel) and [B] the $z = 1.9888$ DLA towards TXS1850+402 (right panel). In both panels, H I 21cm optical depth ($100 \times \tau_{21\text{cm}}$) is plotted against heliocentric frequency, in MHz. The top axis of both panels shows velocity, in km s^{-1} , relative to $z = 1.9698$ (left panel) and $z = 1.9888$ (right panel). In the case of TXS1755+578, the spectrum has been smoothed to, and resampled at, a velocity resolution of $\approx 31 \text{ km s}^{-1}$.

TABLE 1
RESULTS

| QSO | z_{QSO}^A | z_{DLA}^A | N_{HI}^A $\times 10^{21} \text{ cm}^{-2}$ | S_ν^B mJy | $\int \tau dV$ km s^{-1} | ΔV_{90}^C km s^{-1} | f^D | T_s^E K |
|----------|--------------------|--------------------|---|------------------|--------------------------------------|---|-------|----------------|
| 1755+578 | 2.110 | 1.9698 | 2.51 ± 0.15 | 377.4 ± 1.3 | 0.85 ± 0.16 | 41 | 0.15 | — |
| 1850+402 | 2.120 | 1.9888 | 2.00 ± 0.25 | 650.3 ± 3.2 | 2.95 ± 0.14 | 100 | 1.0 | (372 ± 18) |

Notes: (A) The values of z_{QSO} , z_{DLA} and N_{HI} are from Jorgenson et al. (2006).

(B) The flux density S_ν is at the redshifted H I 21cm observing frequency.

(C) ΔV_{90} is the velocity range containing 90% of the integrated H I 21cm optical depth (e.g. Prochaska & Wolfe 1997).

(D) The covering factor f has been estimated from high-frequency VLBI studies; see main text for details.

(E) The DLA spin temperature T_s is not listed for the $z = 1.9698$ DLA towards TXS1755+578 as it appears plausible that the radio and optical sightlines are not the same for this source; see main text for details.

(Henstock et al. 1995; Pollack et al. 2003). In combination with the flat spectrum of TXS1850+402, this suggests that the covering fraction is likely to be close to unity at low frequencies. Conversely, 5 GHz VLBI studies of TXS1755+578 have shown that the source has multiple components extended over 30 mas, with a core flux density of $\approx 58 \text{ mJy}$ and a total flux density of $\approx 396 \text{ mJy}$ in the VLBI image (Pollack et al. 2003; Helmboldt et al. 2007); this suggests a core fraction of ≈ 0.15 . Including these in the spin temperature estimates yields $T_s \approx (242 \pm 46) \times (f/0.15) \text{ K}$ (TXS1755+578) and $T_s \approx (372 \pm 18) \times (f/1.0) \text{ K}$ (TXS1850+402), assuming that the H I 21cm absorption towards TXS1755+578 arises towards the radio core. Both absorbers thus appear to have relatively low T_s values, significantly lower than the typical spin temperatures of high redshift DLAs ($T_s \gtrsim 1000 \text{ K}$; Kanekar et al. 2014). Low-frequency VLBI imaging of the two DLAs will be of much interest to directly estimate the core fraction close to the redshifted H I 21cm line frequencies.

It should be emphasized that it is possible that the detected H I 21cm absorption towards TXS1755+578 arises towards one of the four jet components, and not towards the radio core. This cannot be ruled out, given the weakness of the H I 21cm

absorption as well as the relative weakness of the core compared to the jet components. Further, the core is likely to have a strongly inverted spectrum and is hence likely to be even weaker relatively to the jet components at low frequencies. It is hence plausible that the radio and optical sightlines are not the same for TXS1755+578 (see below). Caution should hence be exercised while interpreting the results towards this source, in the absence of VLBI observations in the redshifted H I 21cm line.

Both DLAs are known to show strong metal-line absorption in their optical spectra, with multiple absorption components (Prochaska & Wolfe 1998; Jorgenson et al. 2010). For TXS1850+402, the redshifts of the two strongest metal-line components are in reasonable agreement with the two H I 21cm absorption components. These components are likely to be arise in cold gas, which gives rise to the H I 21cm absorption; the other metal-line components are likely to originate in warmer gas. Conversely, in the case of TXS1755+578, Jorgenson et al. (2010) found eight C I absorption components in their Keck-Hires spectrum, as well as Si II* absorption. Since C I absorption is expected to arise in cold gas, it may be surprising that the H I 21cm absorption profile towards

TXS1755+578 shows only a single absorption component, which is itself offset in velocity from the stronger C I lines. This too suggests that radio core in TXS1755+578 may be extremely weak at low frequencies, with the H I 21cm absorption arising towards one of the components in the radio jet. As such, one should not use the H I column density determined towards the optical QSO with the H I 21cm optical depth to estimate the absorber spin temperature.

Finally, the DLA towards TXS1850+402 has a relatively high metallicity, $[\text{Zn}/\text{H}] = -0.68 \pm 0.04$ (Prochaska & Wolfe 1998). Its low T_s value is thus consistent with the anti-correlation between metallicity and spin temperature that has been found in DLAs (Kaneekar et al. 2009c; Ellison et al. 2012; Kaneekar et al. 2014). The DLA towards TXS1755+578 has an even higher metallicity, $[\text{Zn}/\text{H}] = -0.25 \pm 0.19$ (Jorgenson et al. 2010, Jorgenson et al., in prep.). While this too is consistent with a large cold gas fraction and hence a low DLA spin temperature, the likely difference between the radio and optical sightlines in this absorber implies that one cannot test the anti-correlation between metallicity and spin temperature here.

In summary, I report the detection of redshifted H I 21cm absorption in two DLAs at $z \approx 2$ towards TXS1755+578 and TXS1850+402 with a new wide-band GMRT receiver that covers 250 – 500 MHz, with integrated H I 21cm optical depths of $\int \tau_{21\text{cm}} dV = (0.85 \pm 0.16) \text{ km s}^{-1}$ (TXS1755+578) and $\int \tau_{21\text{cm}} dV = (2.95 \pm 0.14) \text{ km s}^{-1}$ (TXS1850+402). These are only the eighth and ninth detections of H I 21cm absorption in DLAs at $z \gtrsim 2$. For the $z = 1.9888$ DLA towards TXS1850+402, the compact nature of the background source (with size $\approx 1.4 \text{ mas}$ at 5 GHz) suggests that the low-frequency covering factor is close to unity. Combining the H I column density measured from the Lyman- α line with the H I 21cm optical depth then yields a spin tem-

perature $T_s = (372 \pm 18) \times (f/1.0) \text{ K}$. This low T_s value and the relatively high DLA metallicity are consistent with the anti-correlation between the two quantities that has been earlier found in DLAs. In the case of the $z = 1.9698$ absorber towards TXS1755+578, the weakness of the radio core and the fact that the profiles in the H I 21cm and C I lines are very different suggest that the radio and optical absorption arise from different sightlines, and hence, that one should not attempt to combine the two to infer a spin temperature. The detection of two new H I 21cm absorbers in the commissioning phase of the new wide-band GMRT receivers, and with only one-third the collecting area of the full GMRT, indicate that both the number of detections of H I 21cm absorption and our understanding of physical conditions in the neutral gas in high- z DLAs are likely to improve significantly in the next few years.

It is a pleasure to thank Hanumanth Rao Bandari, Jayaram Chengalur, Yashwant Gupta, Shilpa Dubal, Santaji Katore, Navnath Shinde, Rupsingh Vasave, Nilesh Raskar, Deepak Bhong and Manisha Jangam for many discussions on the new GMRT receivers and much help with the observations. I also thank Regina Jorgenson for providing, in advance of publication, the metallicity of the DLA towards TXS1755+578, and Jayaram Chengalur, Maryam Arabsalmani, and an anonymous referee for comments on an earlier version of the manuscript. Finally, I thank the staff of the GMRT who have made these observations possible. The GMRT is run by the National Centre for Radio Astrophysics of the Tata Institute of Fundamental Research. I acknowledge support from the Department of Science and Technology, India, via a Ramanujan Fellowship.

REFERENCES

- Bandari, H. R., Sankarasubramanian, G., & Praveen Kumar, A. 2013, IOP Conf. Ser.: Mater. Sci. Eng., 44, 012023
- Braun, R. & Walterbos, R. 1992, *ApJ*, 386, 120
- Briggs, F. H., Brinks, E., & Wolfe, A. M. 1997, *AJ*, 113, 467
- Briggs, F. H. & Wolfe, A. M. 1983, *ApJ*, 268, 76
- Carilli, C. L., Lane, W. M., de Bruyn, A. G., Braun, R., & Miley, G. K. 1996, *AJ*, 111, 1830
- Chengalur, J. N. & Kaneekar, N. 2000, *MNRAS*, 318, 303
- de Bruyn, A. G., O’Dea, C. P., & Baum, S. A. 1996, *A&A*, 305, 450
- Dickey, J. M., Terzian, Y., & Salpeter, E. E. 1978, *ApJS*, 36, 77
- Ellison, S. L., Kaneekar, N., Prochaska, J. X., Momjian, E., & Worseck, G. 2012, *MNRAS*, 424, 293
- Ellison, S. L., Yan, L., Hook, I. M., Pettini, M., Wall, J. V., & Shaver, P. 2001, *A&A*, 379, 393
- Ellison, S. L., York, B. A., Pettini, M., & Kaneekar, N. 2008, *MNRAS*, 388, 1349
- Gupta, N., Srianand, R., Petitjean, P., Bergeron, J., Noterdaeme, P., & Muzahid, S. 2012, *A&A*, 544, 21
- Gupta, N., Srianand, R., Petitjean, P., Khare, P., Saikia, D. J., & York, D. G. 2007, *ApJ*, 654, L111
- Gupta, N., Srianand, R., Petitjean, P., Noterdaeme, P., & Saikia, D. J. 2009, *MNRAS*, 398, 201
- Heimboldt, J. F., Taylor, G. B., Tremblay, S., Fassnacht, C. D., Walker, R. C., Myers, S. T., Sjouwerman, L. O., Pearson, T. J., Readhead, A. C. S., Weintraub, L., Gehrels, N., Romani, R. W., Healey, S., Michelson, P. F., Blandford, R. D., & Cotter, G. 2007, *ApJ*, 658, 203
- Henstock, D. R., Browne, I. W. A., Wilkinson, P. N., Taylor, G. B., Vermeulen, R. C., Pearson, T. J., & Readhead, A. C. S. 1995, *ApJS*, 100, 1
- Jorgenson, R. A., Wolfe, A. M., & Prochaska, J. X. 2010, *ApJ*, 722, 460
- Jorgenson, R. A., Wolfe, A. M., Prochaska, J. X., Lu, L., Howk, J. C., Cooke, J., Gawiser, E., & Gelino, D. M. 2006, *ApJ*, 646, 730
- Kaneekar, N. & Briggs, F. H. 2004, *New Astr. Rev.*, 48, 1259
- Kaneekar, N. & Chengalur, J. N. 1997, *MNRAS*, 292, 831
- . 2001, *A&A*, 369, 42
- . 2003, *A&A*, 399, 857
- Kaneekar, N., Chengalur, J. N., & Lane, W. M. 2007, *MNRAS*, 375, 1528
- Kaneekar, N., Ellison, S. L., Momjian, E., York, B., & Pettini, M. 2013, *MNRAS*, 428, 532
- Kaneekar, N., Lane, W. M., Momjian, E., Briggs, F. H., & Chengalur, J. N. 2009a, *MNRAS*, 394, L61
- Kaneekar, N., Prochaska, J. X., Ellison, S. L., & Chengalur, J. N. 2009b, *MNRAS*, 396, 385
- . 2010, *ApJ*, 712, L148
- Kaneekar, N., Prochaska, J. X., Smette, A., Ellison, S. L., Ryan-Weber, E. V., Momjian, E., Briggs, F. H., Lane, W. M., Chengalur, J. N., Delafosse, T., Grave, J., Jacobsen, D., & de Bruyn, A. G. 2014, *MNRAS*, 438, 2131
- Kaneekar, N., Smette, A., Briggs, F. H., & Chengalur, J. N. 2009c, *ApJ*, 705, L40
- Kaneekar, N., Subrahmanyam, R., Ellison, S. L., Lane, W. M., & Chengalur, J. N. 2006, *MNRAS*, 370, L46
- Lane, W., Smette, A., Briggs, F., Rao, S., Turnshek, D., & Meylan, G. 1998, *AJ*, 116, 26
- Lane, W. M. & Briggs, F. H. 2002, *ApJ*, 561, L27
- Noterdaeme, P., Ledoux, C., Petitjean, P., & Srianand, R. 2008, *A&A*, 481, 327
- Pettini, M., Smith, L. J., Hunstead, R. W., & King, D. L. 1994, *ApJ*, 426, 79
- Pollack, L. K., Taylor, G. B., & Zavala, R. T. 2003, *ApJ*, 589, 733
- Prochaska, J. X., Gawiser, E., Wolfe, A. M., Castro, S., & Djorgovski, S. G. 2003, *ApJ*, 595, L9
- Prochaska, J. X., Wolfe, A. M., 1997, *ApJ*, 487, 73
- Prochaska, J. X. & Wolfe, A. M. 1998, *ApJ*, 507, 113
- Rafelski, M., Wolfe, A. M., Prochaska, J. X., Neeleman, M., & Mendez, A. J. 2012, *ApJ*, 755, 89
- Rahmani, H., Srianand, R., Gupta, N., Petitjean, P., Noterdaeme, P., & Vázquez, D. A. 2012, *MNRAS*, 425, 556
- Rao, S. M. & Turnshek, D. A. 2000, *ApJS*, 130, 1

- Rao, S. M., Turnshek, D. A., & Nestor, D. B. 2006, ApJ, 636, 610
- Rohlfs, K. & Wilson, T. L. 2006, Tools of Radio Astronomy, 4th ed. (Berlin: Springer)
- Srianand, R., Gupta, N., Petitjean, P., Noterdaeme, P., Ledoux, C., Salter, C. J., & Saikia, D. J. 2012, MNRAS, 421, 651
- Wolfe, A. M., Briggs, F. H., & Davis, M. M. 1982, ApJ, 259, 495
- Wolfe, A. M., Briggs, F. H., Turnshek, D. A., Davis, M. M., Smith, H. E., & Cohen, R. D. 1985, ApJ, 294, L67
- Wolfe, A. M., Brown, R. L., & Roberts, M. S. 1976, Phys. Rev. Lett., 37, 179
- Wolfe, A. M. & Davis, M. M. 1979, AJ, 84, 699
- Wolfe, A. M., Gawiser, E., & Prochaska, J. X. 2005, ARA&A, 43, 861
- York, B. A., Kanekar, N., Ellison, S. L., & Pettini, M. 2007, MNRAS, 382, L53